EUROPEAN COMMISSION
Community Research

SEVENTH FRAMEWORK PROGRAMME

ARCHER

Collaborative Project (CP)

Co-funded by the European Commission under the Euratom Research and Training Programme on Nuclear Energy within the Seventh Framework Programme

Grant Agreement Number : 269892

Start date : 01/02/2011 Duration : 48 Months
www.archer-project.eu

Structural and chemical characterization of B4C- and Ag-SiC-coated ceramic microparticles

Authors : FUTTERER Michael (JRC) , Ana Ruiz (JRC), Martin Lustfeld (TUD), Anne-Maria Reinecke (TUD)

ARCHER - Contract Number: 269892
Advanced High-Temperature Reactors for Cogeneration of Heat and Electricity R&D
EC Scientific Officer: Dr. Panagiotis Manolatos

Document title	Structural and chemical characterization of B4C- and Ag-SiC-coated ceramic microparticles
Author(s)	FUTTERER Michael (JRC), Ana Ruiz (JRC), Martin Lustfeld (TUD), Anne-Maria Reinecke (TUD)
Number of pages	30
Document type	Deliverable
Work Package	WP 31
Document number	D31.33
Issued by	JRC
Date of completion	23/01/2015
Dissemination level	Confidential, only for members of the consortium (including the Commission Services).

Summary

The subproject Fuel in the FP7 ARCHER project on High and Very High Temperature Technology evaluates the feasibility of a new type of separate effect irradiation test on TRISO coated fuel particles. Such an irradiation test should investigate the individual effect of internal pressurization on the mechanical properties of coatings and study the diffusion of Ag across the coatings. The present study represents a key step in the feasibility assessment of such an irradiation test. Two rounds of particles coated by pulsed laser deposition (PLD) at Technische UniversitÃ¤t Dresden have been characterized by SEM, EDX, XRD and CT. Each round consisted of eight batches of B4C- and SiC-coated microparticles. The first round of batches produced coatings with a low thickness and poor stoichiometry (B/C or Si/C ratios), in particular in the case of the SiC layers. The thorough analysis of the first round gave insights on how to significantly enhance the coating process. Taking into consideration these findings, the PLD coating process was optimized and as surrogate kernels both ZrO2 and buffer/PyC-coated particles were used. The second round of batches was of much higher quality with respect to stoichiometry, layer thickness, layer adherence and, in the case of SiC, layer hermetical properties for Ag retention.

Approval

Date	By
23/01/2015	Steven KNOL
29/01/2015	Mathias LAURIE
29/01/2015	Steven KNOL

Distribution list

Name	Organisation	Comments
P. Manolatos	EC DG RTD	Through the EC participant portal
All beneficiaries	ARCHER	Through the private online workspace

EUROPEAN COMMISSION
Directorate General Joint Research Centre
Institute for Energy and Transport – Unit F.04

23 September 2014
PUBSY JRC 91896

JRC TECHNICAL REPORT

Structural and chemical characterization of B_4C- and Ag-SiC-coated ceramic microparticles

rev. 0

Deliverable D31.33 for the FP7 ARCHER Project

Contract Number: 269892

A. Ruiz (JRC), M. Lustfeld (TUD), A.-M. Reinecke (TUD), Michael A. Fütterer (JRC)

	For the Authors	Reviewed by	Verified by Contact Person	Approved by Unit Head
Name	A. Ruiz	S. Holmstrom	K. F. Nilsson	P. Hähner
Date	23/09/2014	24/09/2014	29/09/2014	29.9.2014
Signature				

Table of contents

1. Introduction

The FP7 project ARCHER is currently being performed to advance the technology basis of nuclear High and Very High Temperature Reactors. In line with the Sustainable Nuclear Energy Technology Platform's (SNETP) Strategic Research Agenda and Deployment Strategy, ARCHER thus supports the envisaged demonstration of nuclear cogeneration as an effective means to respond to European energy policy targets in terms of climate change, competitiveness and energy security.

Subproject 3 of the ARCHER project is dedicated to better understand the behavior of coated particle fuel under irradiation. A specific task is dedicated to verify the technical feasibility of a new type of separate effect irradiation test with particular focus on:

1. **The evolution of mechanical properties of coated particles under irradiation at high temperature and with increasing internal pressure due to fission product and He build-up:**

   For these tests, the use of a surrogate (i.e. no fuel containing) kernel with a suitable boron compound (e.g. B_4C) on the kernel is envisaged. The boron will generate a significant amount of He during irradiation that creates large internal pressures on the load bearing layers thus simulating the pressure build-up in real fuel. The kernels were provided by Manchester University and coated with B_4C at Technical University Dresden using pulsed laser deposition (PLD). The benefit of PLD technology is the very low temperature-load during the coating process, and the very high adhesive strength of the generated layers. After B_4C coating, the resulting particles will be overcoated with conventional TRISO layers at Manchester University by fluidized bed chemical vapor deposition (FBCVD). In this study, the feasibility of the process was tested, and the quality of the particles determined. The result is a very novel type of samples, which can provide insight in the coating behavior under different pressure, neutron flux and temperature conditions. Once a decision for irradiation is made, the generated data can help validate fuel performance codes for design and licensing purposes.

2. **The diffusion of the radioactive fission product Ag across SiC coatings under irradiation and high temperature.**

   Silver (Ag) is a radioactive fission product which may under certain circumstances diffuse across the SiC layer of coated particle fuel, deposit on graphite or colder parts of the primary cooling circuit and thus create radioactive hot spots which make in-service inspection campaigns long and difficult. To study the diffusion properties of Ag through the coating layers, Ag-SiC multicoatings on surrogate kernels were prepared by PLD at Technical University Dresden to evaluate the Ag retention capability of nanocrystalline SiC in TRISO coatings.

Technical University Dresden has delivered in total 16 batches of coated particles of both sorts to JRC-IET where these particles were then characterized using SEM, EDX, XRD and CT. Feedback from the analysis of the first batches has helped fine-tune the preparation of the

consecutive batches so that the manufacturing capability of particles for the envisaged irradiation test can be confirmed.

1.1. Sample preparation by PLD

Pulsed laser deposition (PLD) was used with the aim of preparing single nanocrystalline B_4C and SiC coatings, as well as multilayer coatings consisting of Ag and SiC, on TRISO-like surrogate kernels. The samples obtained by this process may serve for testing the high-temperature stability of amorphous or nanocrystalline B_4C and SiC. As well, the Ag-SiC multicoatings may be used as diffusion couples to evaluate the Ag retention capability of nanocrystalline SiC in TRISO coatings.

The PLD process was carried out in a test facility of the Technical University of Dresden described in[1] under the conditions detailed in deliverable D.31.31. Briefly, a pulsed excimer laser (Lambda Physics Coherent LPX Pro 305i) with a wavelength of 248 nm and pulse duration of 25 ns, was focused onto the target at an incidence angle of 45° and spot size of 3 mm^2. The pulse repetition rate was set to 40 Hz and the pulse energy to 200 mJ. A rotating crucible was used as kernel holder to ensure a continuous rotational movement of the kernels and, thus, a uniform coating. The distance between the target and the kernels in the crucible was fixed at 50 mm. The kernels were heated by means of a continuous wave diode laser and an infrared camera controlled the kernels temperature. Sintered high-purity 6H-SiC with a density of 3.16 g/cm^3 (ESK Ceramics EKasic F plus) and plain silver were used as target materials. Pressure, heating rate and temperature were adjusted in the reactor chamber for each batch as described in deliverable D.31.31.

[1] Reinecke et al., *Nuc. Eng. Des.*, 2014, **271**, 92.

2. Characterization of the first round of batches

Summary

From the first eight batches of B_4C- and SiC-coated microparticles, three of them (Batches 1 – 3) consisted of B_4C-coated Al_2O_3 and the other five (Batches 4 – 8) consisted of SiC-coated ZrO_2. Table 1 summarizes the main findings of the characterization analysis. From a chemical point of view, the best B_4C coating was found in Batch 2, where the B/C ratio closest to the stoichiometric value of 4 was measured (2.97) and the XRD diffractrogram showed a peak at ~38° that may correspond to B_4C. However, the thickness of this coating was the lowest among the B_4C (650 nm). Batch 1 had also a good B/C ratio (2.8) with a better thickness (3 µm), but the coating was not detected by XRD.

The SiC coatings were very thin (150 ~ 350 nm) with a low Si/C ratio, as measured by EDX, except for Batch 4, where we observed a 40 µm thick layer with a Si/C ratio close to the stoichiometric value of 1 (1.15) and cubic SiC was clearly detected by XRD. However, this batch was done on a core with an external SiC layer and we could not distinguish two SiC layers (one from the core and one from the PLD coating). The other batches (5 – 8) had similar characteristics: coatings of several hundreds of nanometer, Si/C ratios around 0.2 and no trace of the coatings were observed by XRD. Batch 5 was the thinnest (150 nm), but the morphology of the layer was more uniform with less deposits on top of the coating. The buried Ag layer was not successfully trapped underneath the SiC coating, as many Ag particles were found on the surface of SiC.

As conclusion, **Batch 2**, for B_4C, and **Batch 4**, for SiC, present the most promising crystallographic characteristics among the first round of coatings: better B/C or Si/C atomic ratio, lower porosity, and boron carbide and silicon carbide phases probably detected by XRD.

Table 1. Layer thickness and stoichiometry of the first round of coatings

coating	B_4C			Ag - SiC				
core	Al_2O_3			C/SiC - coated ZrO_2	ZrO_2			
Batch	**1**	**2**	**3**	**4**	**5**	**6**	**7**	**8**
Particle size (µm)	545	465	510	865	480	490	510	510
Layer thickness (µm)	3	0.65	4	40	0.15	0.3	0.3	0.35
B/C (EDX)	2.80	2.97	2.77	-	-	-	-	-
Si/C (EDX)	-	-	-	1.15	0.19	0.2	0.17	0.23

2.1. Morphology

The morphology of the particles was characterized by SEM. Figures 1-3 show SEM images of the outer surface of the B_4C and SiC coatings. Regarding B_4C coatings (Figure 1), Batches 1 and 3 presented a more porous layer than Batch 2 and the coating seemed to be thicker. The coating of Batch 2 was more compacted and less homogeneous, presenting regions with low porosity and other regions with higher porosity (white arrows in Figure 1c).

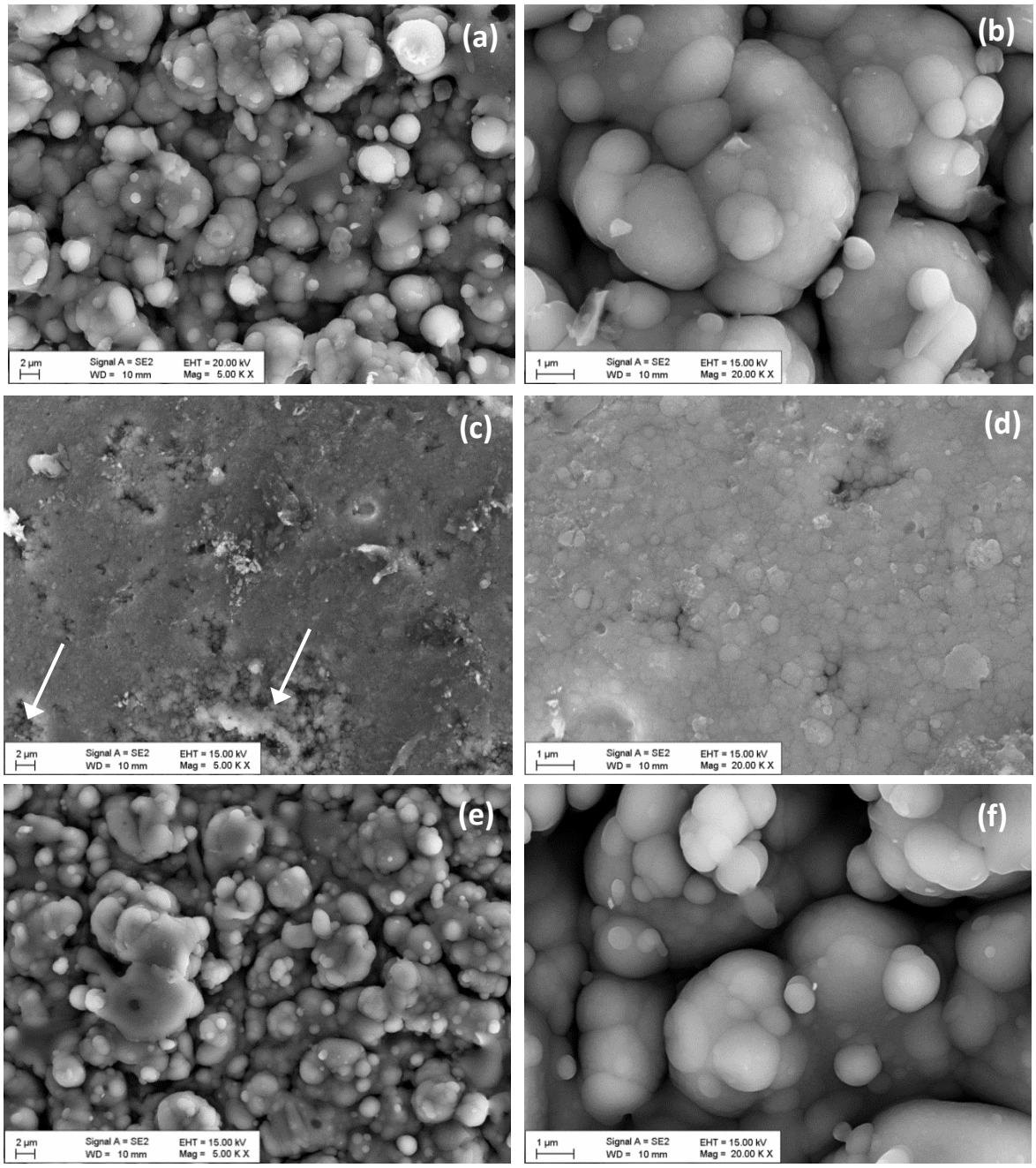

Figure 1. SEM images of B_4C coatings. Batches 1 (a,b), 2 (c,d) and 3 (e,f).

Concerning SiC coatings (Figures 2 and 3), Batch 4 had a distinct morphology as compared to the other batches. The surface presents two grain size distributions: bigger grains (~2µm) surrounded by smaller grains (~100nm). The bigger grains might be formed by the coalescence of the smaller ones, or it can be that they belong to the external SiC layer of the particle core. The other SiC coatings presented a similar morphology: smoother surface and small grains. In batches 6 to 8 the surface exhibited some holes (see Fig. 3f), which might be from the zirconia core and suggest that the coating is very thin. The coatings 5 to 8 exhibited also some bubbles that may cause fragility of the layer and could be sites where cracks initiate (see Fig. 3e as example). It was also noticed that these batches presented some deposits on top of the coating, particularly in Batch 6 (see arrows in Figure 3a).

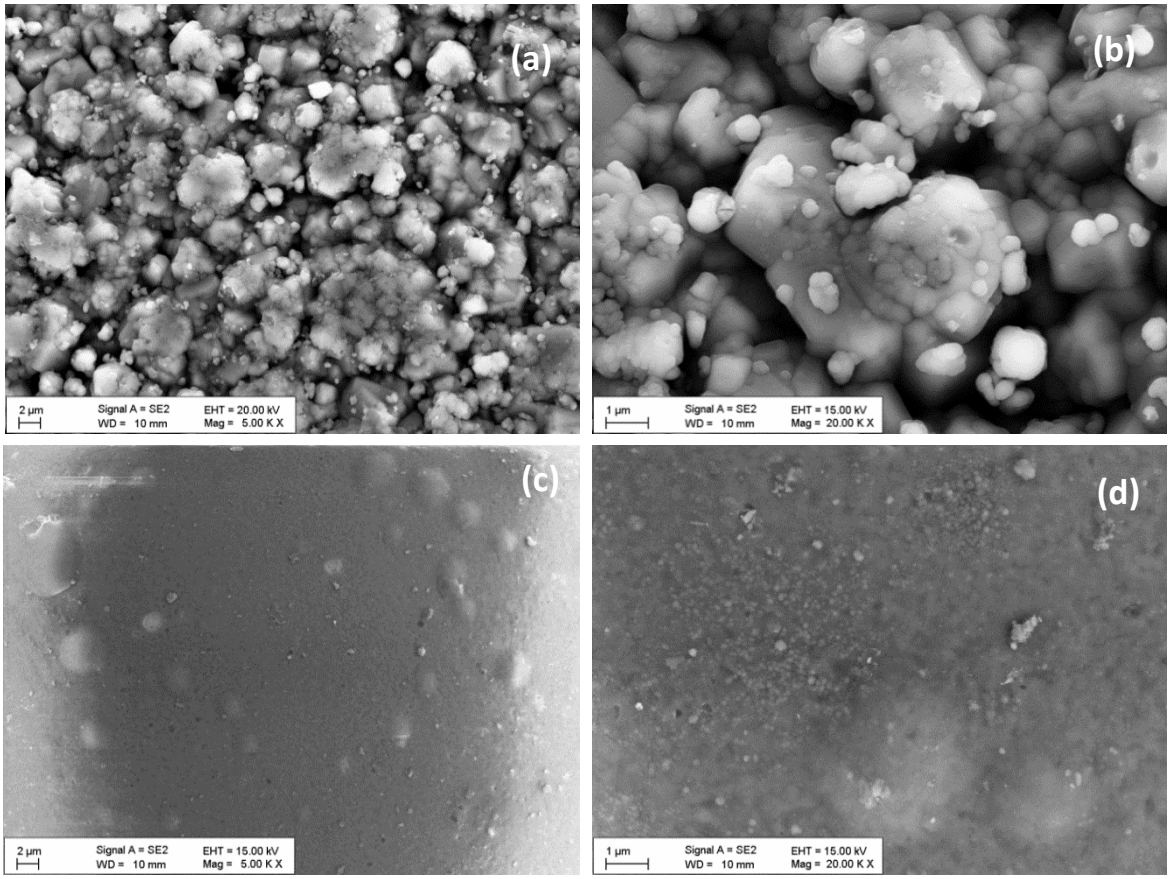

Figure 2. SEM images of SiC coatings. Batches 4 (a, b) and 5 (c,d).

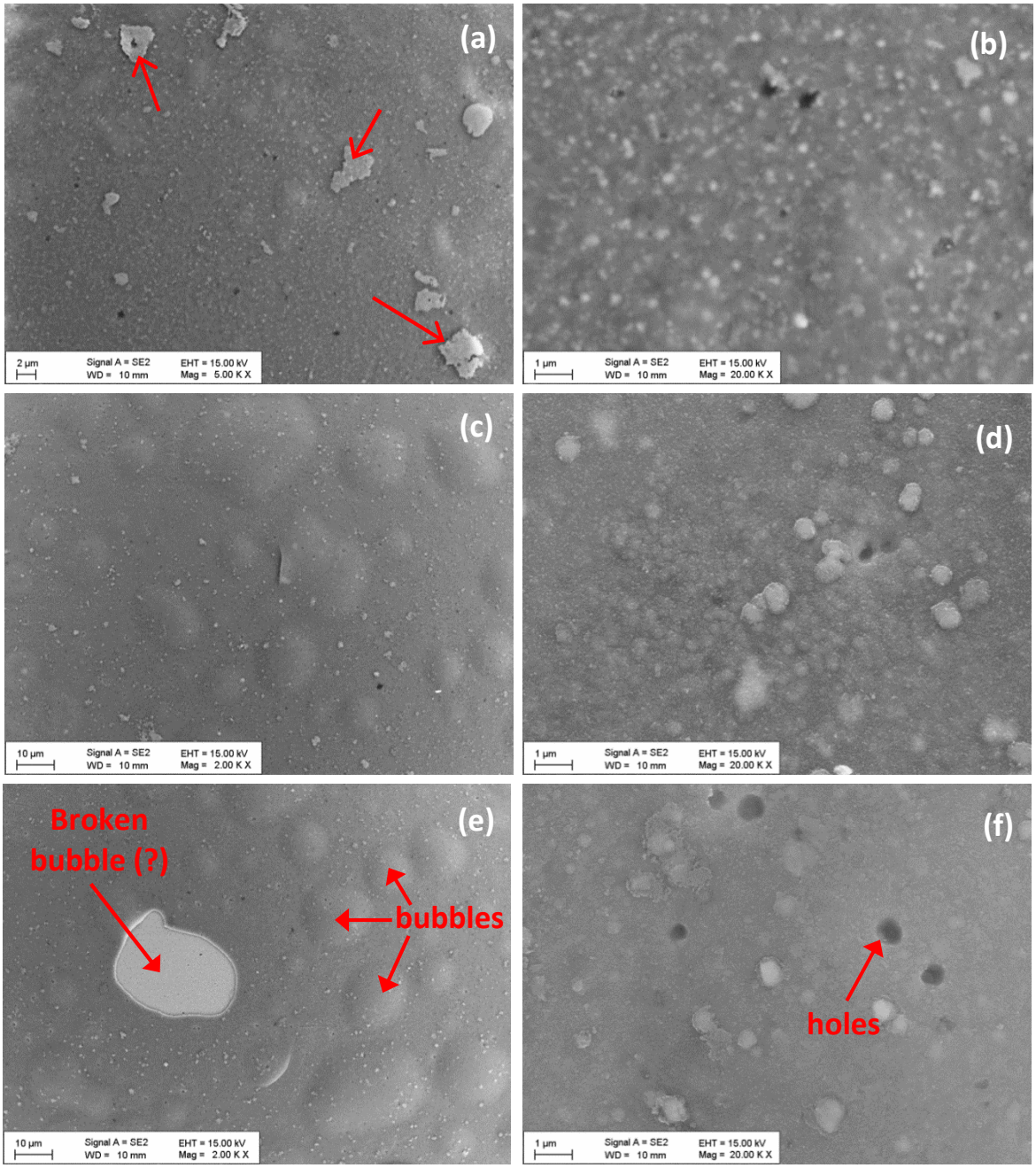

Figure 3. SEM images of SiC coatings. Batches 6 (a, b), 7 (c, d) and 8 (e, f). Arrows in Batch 6 indicate deposits on top of the coating.

2.2. Layer thickness

To measure the thickness of the layers, the particles were either broken or embedded in resin, cut and polished. Smaller thicknesses than expected were measured (see deliverable D.31.31 for details on the coating process). Figures 4 and 5 show the cross sections of the B_4C and SiC coatings, respectively. EDX was performed at different points of the cross-sections to identify the extension of the coating. Batches 1 and 3 had a B_4C layer of thickness between 3 and 4 µm. However, the layer of batch 2 was only 650 nm thick.

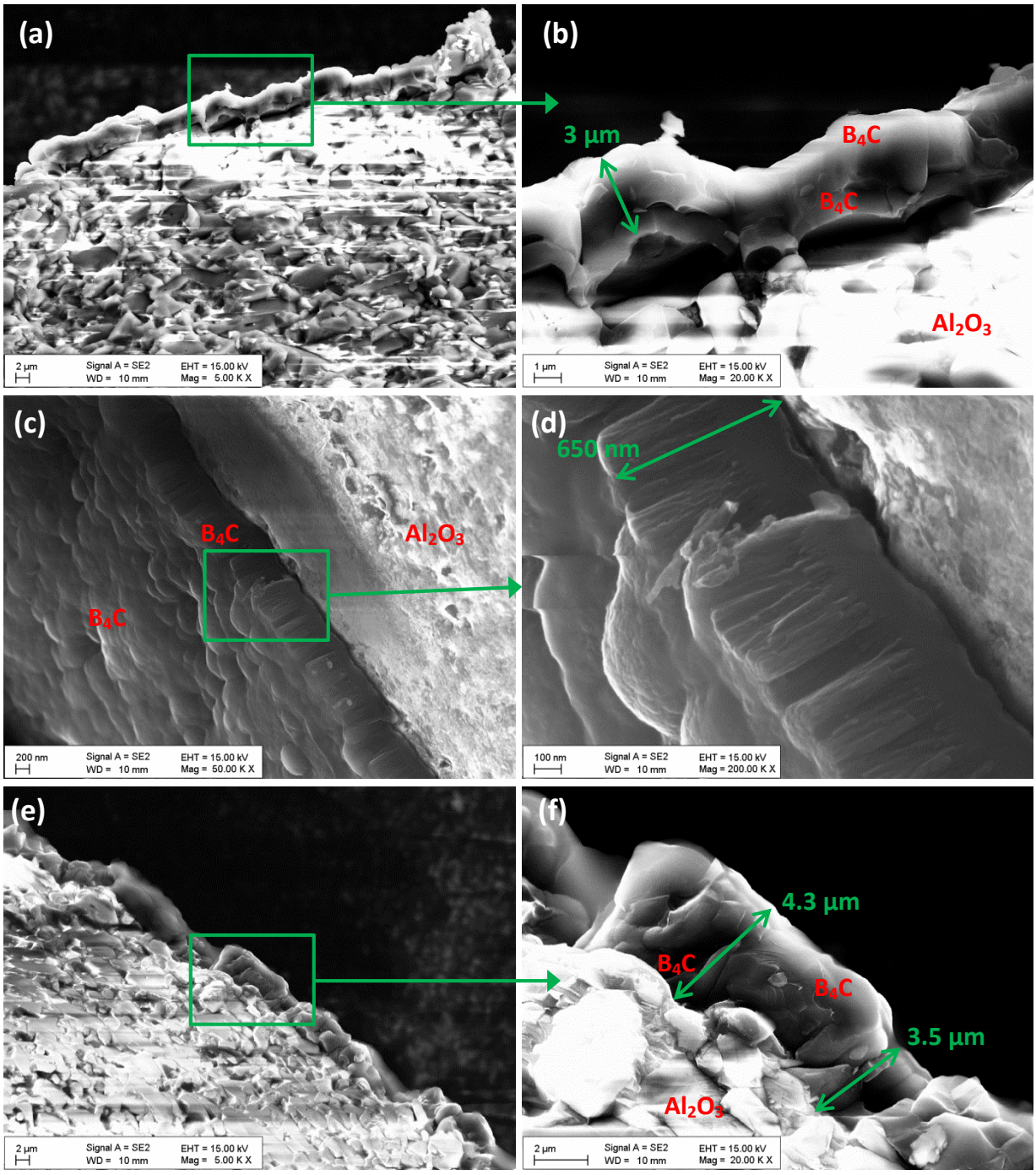

Figure 4. Thickness of B_4C coatings. Batches 1 (a,b), 2 (c,d) and 3 (e,f). The red labels indicate the points where EDX was carried out to discern the extension of the coating.

The thickest SiC coating was found in Batch 4 (40 µm) and the thinnest in batch 5 (only 150 nm). Batches 6, 7 and 8 had thicknesses of around 300nm. However, the major part of the SiC layer of Batch 4 was not deposited by PLD, but by a CVD process at University of Manchester, as described in detail in deliverable D.31.31. No trace of Ag was found in the 40 µm thick layer.

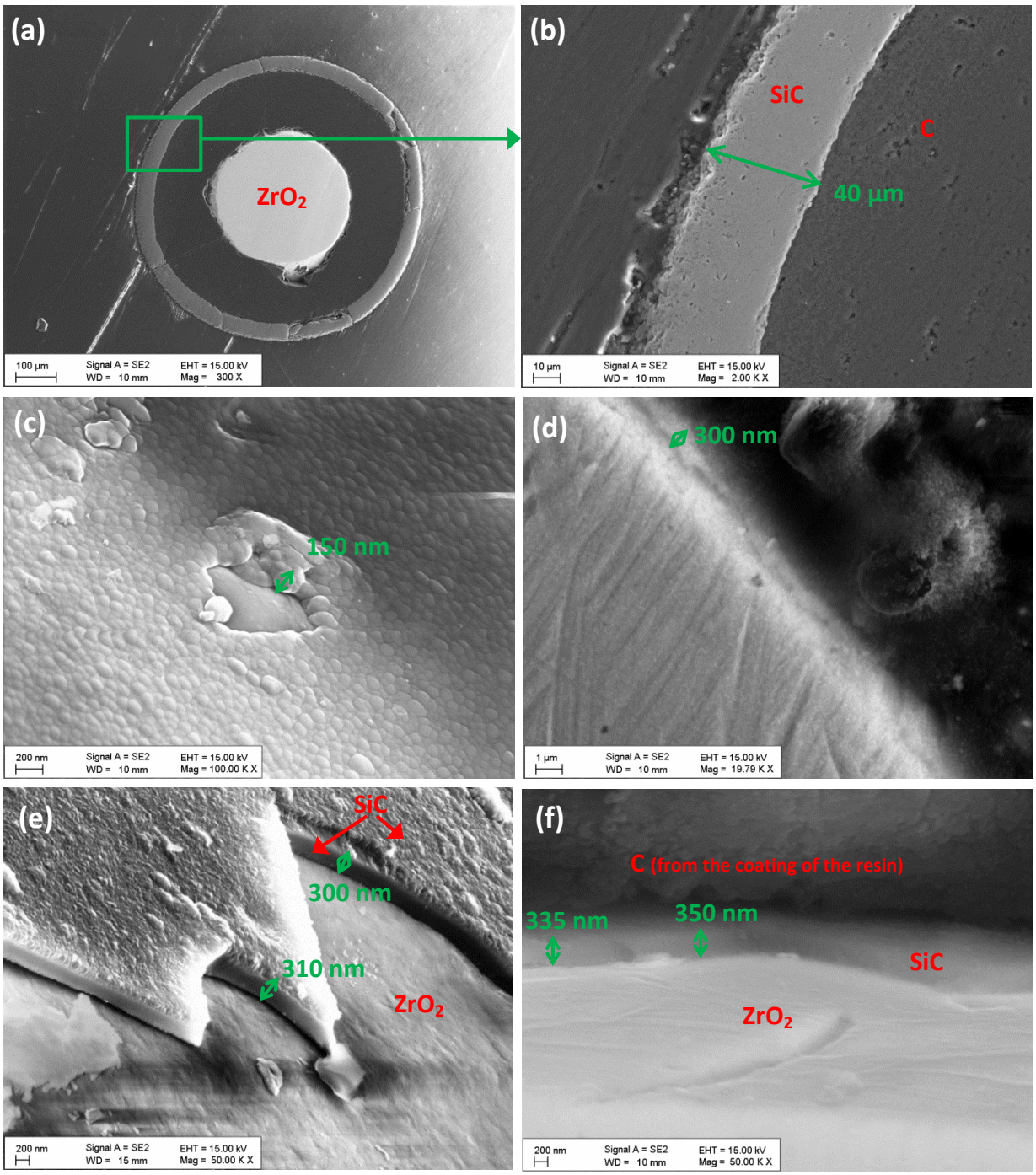

Figure 5. Thickness of SiC coatings. Batches 4 (a,b), 5 (c), 6 (d), 7 (e) and 8 (f). The red labels indicate the points where EDX was carried out.

2.3. Chemical composition.

Light elements, such as B, C or O, are difficult to measure by EDX due to their low photon energies and low fluorescence yield. In addition, the quantification of carbon is delicate because it is a usual contamination element in holders and in the microscope chamber. We tried to decrease the acceleration voltage in EDX in order to resolve better the peaks at low energies, but the deadtime was very low and finally EDX analysis were carried out at 20 kV in all samples.

2.3.1. B_4C-coated Al_2O_3 particles (batches 1-3).

Figure 6 shows the composition of the three batches measured by EDX in a field of view of the same dimensions for each sample. The best B/C ratio was observed in Batch 2 (B/C = 2.97). A more detailed analysis of the three batches in different regions is shown in Figures 7-9.

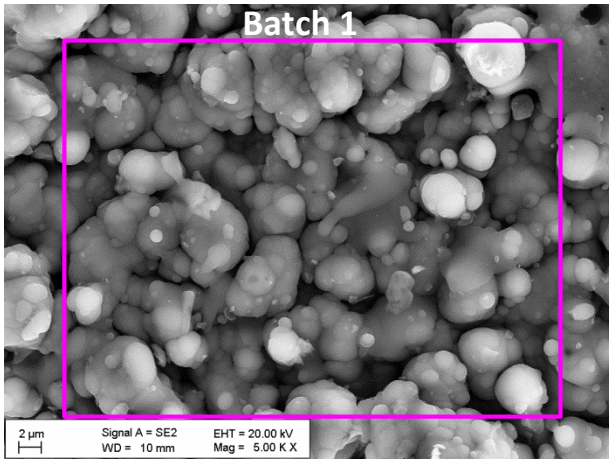

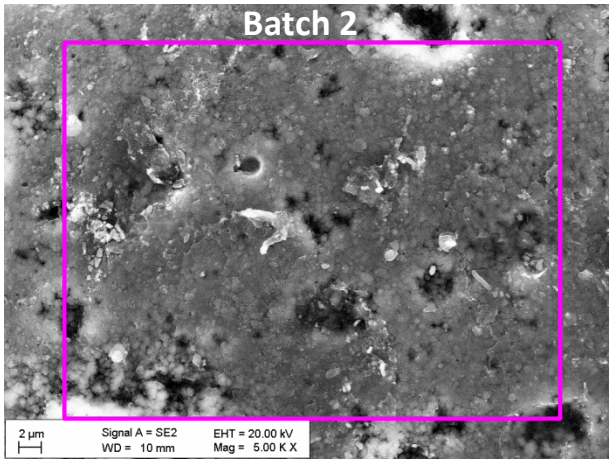

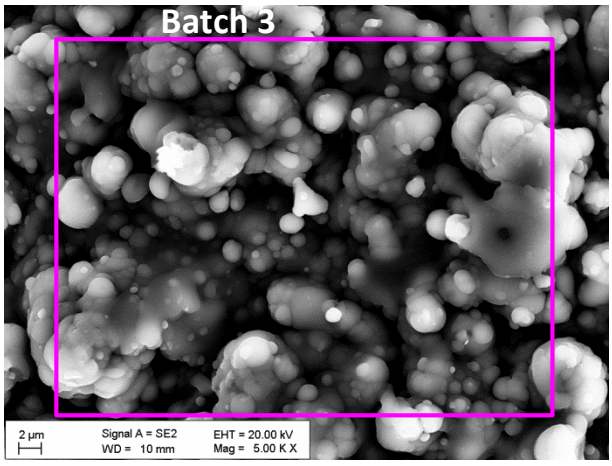

	Composition (at.%)						
	B	**C**	**O**	**Al**	**Si**	**B/C**	**O/Al**
Batch 1	67.13	23.99	7.70	0.80	0.33	**2.80**	**9.63**
Batch 2	64.71	21.82	6.06	7.41	-	**2.97**	**0.82**
Batch 3	67.68	24.45	7.06	0.39	0.33	**2.77**	**18.10**

Figure 6. Composition and B/C atomic ratio of Batches 1, 2 and 3, in at.%

Batch 1

A small peak of Si was detected in this batch, which might come from contamination from the handling with tweezers, but does not affect the relative concentration of the elements of interest. The B/C ratio was similar in the different regions (~ 2.8), except in areas with coarsened particles (Spectrum 3) that presented a slightly poorer stoichiometry.

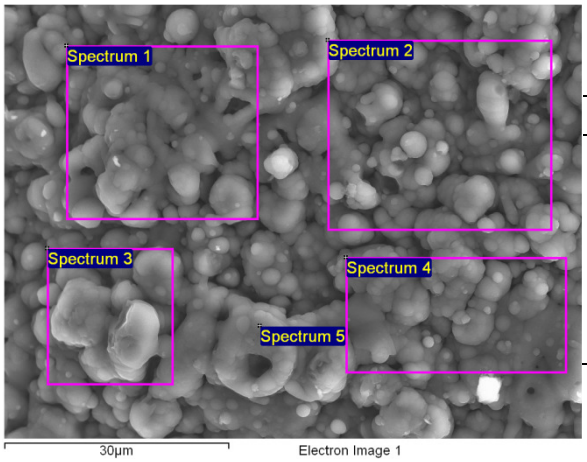

	Composition Batch 1 (at.%)						
	B	**C**	**O**	**Al**	**Si**	**B/C**	**O/Al**
Spectrum 1	67.69	23.76	7.63	0.56	0.31	**2.85**	**13.63**
Spectrum 2	67.92	23.50	7.32	0.83	0.37	**2.89**	**8.82**
Spectrum 3	64.05	27.24	7.82	0.59	0.26	**2.35**	**13.25**
Spectrum 4	68.42	23.05	7.27	0.76	0.42	**2.97**	**9.57**
Spectrum 5	67.48	24.71	7.47	0.14	0.21	**2.73**	**53.36**

Figure 7. Composition and B/C atomic ratio of Batch 1 at different regions, in at.%.

Batch 2

Homogeneous regions present a better B/C ratio (Spectra 1, 3 and 4). In the regions where the nanograins are more pronounced (more porous regions, as in spectrum 2) the B/C ratio is decreased. The less structure is discernible (i.e. in region 4), the better the B/C ratio (3.19).

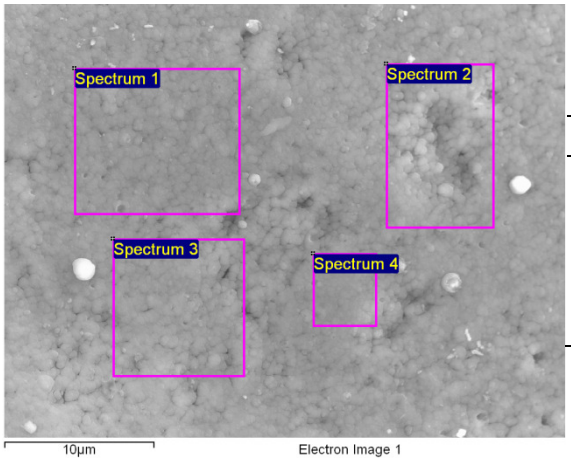

	Composition Batch 2 (at.%)					
	B	**C**	**O**	**Al**	**B/C**	**O/Al**
Spectrum 1	67.08	22.45	6.21	7.26	2.99	0.86
Spectrum 2	63.79	22.93	5.87	7.41	2.78	0.79
Spectrum 3	64.92	21.79	5.94	7.36	2.98	0.81
Spectrum 4	66.19	20.74	5.81	7.25	3.19	0.80

Figure 8. Composition and B/C atomic ratio of Batch 2 at different regions, in at.%.

Batch 3

The B/C ratio is similar in the different regions. The darker, flatter areas (Spectrum 2) were slightly richer in boron and gave a better B/C ratio (2.98), similar to the ratio of Batch 2.

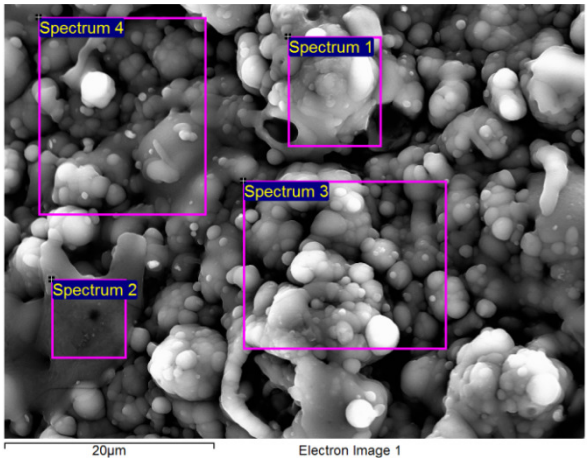

	Composition Batch 3 (at.%)						
	B	**C**	**O**	**Al**	**Si**	**B/C**	**O/Al**
Spectrum 1	66.72	25.92	6.68	0.28	0.33	**2.57**	**23.86**
Spectrum 2	72.66	24.36	2.68	0.12	0.18	**2.98**	**22.33**
Spectrum 3	65.71	26.51	7.19	0.30	0.29	**2.48**	**23.97**
Spectrum 4	67.28	25.44	6.72	0.29	0.26	**2.64**	**23.17**

Figure 9. Composition and B/C atomic ratio of Batch 3 at different regions, in at.%.

2.3.2. SiC-coated ZrO_2 particles (batches 4-8).

Figures 10-14 show the different regions for each batch where EDX analyses had been carried out. The best Si/C ratio was observed in Batch 4 (Si/C ratio close to 1). The other batches had a SiC ratio of around 0.2. Ag was detected on the surface of batches 5 to 8 at atomic concentration of between 0.1 (for Batch 8) and 0.5 (for Batch 5), which indicates that silver has diffused through the SiC coating. Ag appears quite uniformly distributed within the coating, but some bright Ag agglomerates are also seen on the surface. Because of the small thickness of the layers in batches 5 – 8, the x-rays generation extends to a region well underneath the coating and strong peaks of the core elements (Zr, O) are detected.

Batch 4

Due to the thick layer (40 µm) and intermediate carbon layer we did not measure any Zr coming from the core. However, O was detected and could originate from oxidation of the SiC.

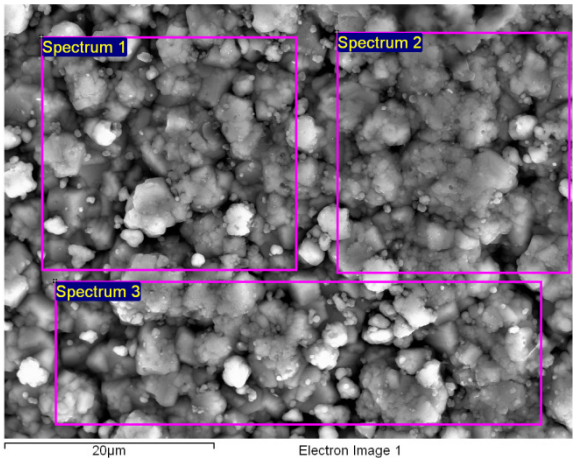

	Composition Batch 4 (at.%)			
	C	**O**	**Si**	**Si/C**
Spectrum 1	39.92	14.20	45.88	**1.15**
Spectrum 2	41.73	13.43	44.84	**1.07**
Spectrum 3	38.51	14.11	47.38	**1.23**

Figure 10. Composition and Si/C atomic ratio of Batch 4 at different regions, in at.%.

Batch 5

Bright particles, as seen in spectrum 5, were rich in Ag. Such particles also gave a higher Si/C ratio than the average of the other regions.

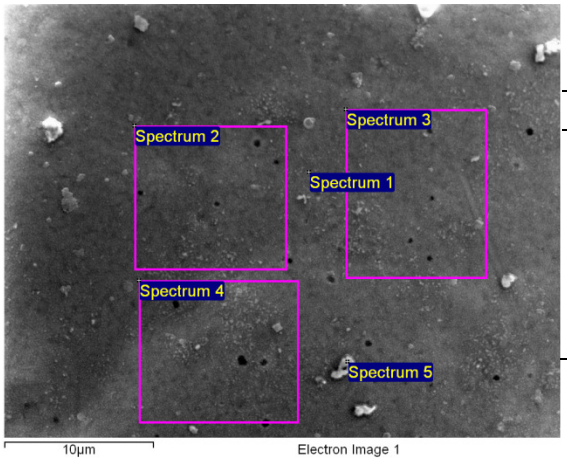

	Composition Batch 5 (at.%)						
	C	**O**	**Si**	**Zr**	**Ag**	**Si/C**	**O/Zr**
Spectrum 1	42.00	37.31	7.62	12.50	0.56	**0.18**	**2.98**
Spectrum 2	41.08	38.24	7.33	12.59	0.49	**0.18**	**3.04**
Spectrum 3	41.05	37.41	7.82	13.04	0.47	**0.19**	**2.87**
Spectrum 4	40.08	38.26	7.54	13.22	0.59	**0.19**	**2.89**
Spectrum 5	37.88	29.77	9.38	15.92	**7.05**	**0.25**	**1.87**

Figure 11. Composition and Si/C atomic ratio of Batch 5 at different regions, in at.%.

Batch 6

The deposits on the top of the coating (spectra 3 and 4) had a similar composition as the coating. The only difference was a slight decrease in the Ag content.

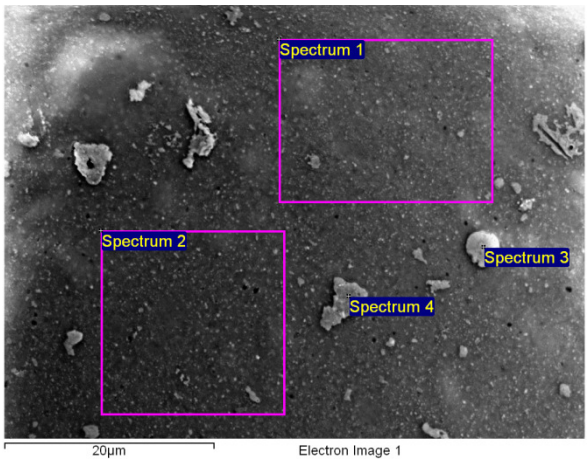

	Composition Batch 6 (at.%)						
	C	**O**	**Si**	**Zr**	**Ag**	**Si/C**	**O/Zr**
Spectrum 1	36.14	45.48	7.5	10.53	0.34	**0.21**	**4.32**
Spectrum 2	36.63	45.33	7.22	10.46	0.36	**0.20**	**4.33**
Spectrum 3	37.84	43.89	7.52	10.52	0.22	**0.20**	**4.17**
Spectrum 4	36.45	45.80	7.30	10.22	0.23	**0.20**	**4.48**

Figure 12. Composition and Si/C atomic ratio of Batch 6 at different regions, in at.%.

Batch 7

The Si/C ratio of batch 7 was, on average, the lowest one. The bright particles (spectrum 4) are rich in Ag.

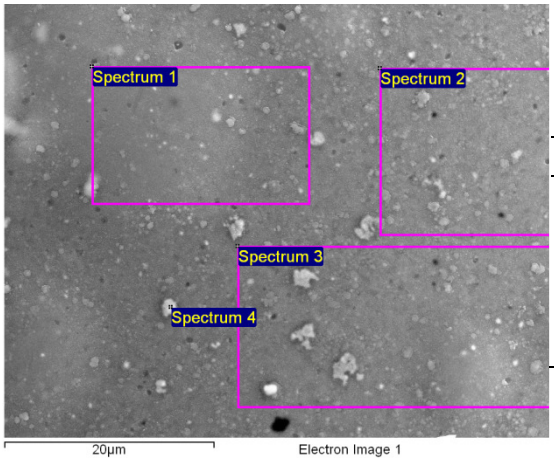

	Composition Batch 7 (at.%)						
	C	**O**	**Si**	**Zr**	**Ag**	**Si/C**	**O/Zr**
Spectrum 1	60.46	20.94	9.36	9.04	0.20	0.15	2.32
Spectrum 2	60.71	19.33	10.26	9.33	0.22	0.17	2.07
Spectrum 3	60.29	19.22	10.56	9.5	0.32	0.18	2.02
Spectrum 4	53.17	21.16	12.86	6.60	**6.20**	0.24	3.21

Figure 13. Composition of Batch 7 at different regions, in wt.% (top table) and at.% (bottom).

Batch 8

The region where the layer was detached (possibly due to crack extension in bubbles as mentioned before) was mainly composed of zirconia.

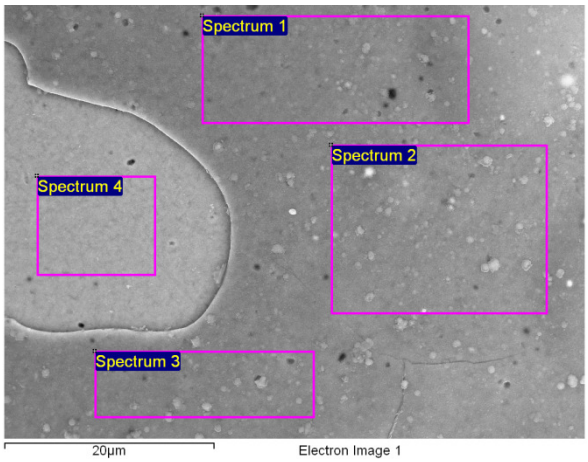

	Composition Batch 8 (at.%)						
	C	**O**	**Si**	**Zr**	**Ag**	**Si/C**	**O/Zr**
Spectrum 1	57.34	21.07	12.44	9.07	0.09	**0.22**	**2.32**
Spectrum 2	56.51	20.09	13.88	9.40	0.11	**0.25**	**2.14**
Spectrum 3	57.75	19.75	13.23	9.16	0.10	**0.23**	**2.16**
Spectrum 4	52.34	31.42	2.39	13.85		**0.05**	**2.27**

Figure 14. Composition and Si/C atomic ratio of Batch 8 at different regions, in at.%.

2.4. Phase analysis by XRD

The main problem to catch the diffraction peaks from the coatings was related to the small thickness, the small number of particles available for studies, and the difficulty in mounting the

material in the sample holder. With a zero-background substrate and a fixed incident length of 20mm, we could register peaks from the particles, but with poor signal-to-noise ratio.

Figure 15a shows the diffraction patterns of the three batches of B_4C-coated alumina particles. In all cases, peaks from rhombohedral alumina (ref. pattern 42-1468) are present. The broad peak at around 44° comes from the zero-background holder and might be due to carbon contamination. Comparing batches 1 and 3 to batch 2, we can see that there is one intense peak at $2\theta \approx 38.0°$ that appears only in batch 2. This could correspond to B_4C since the main diffraction of B_4C is at $2\theta = 37.8°$ (ref. pattern 35-0798 for rhombohedral boron carbide), but it coincides with a low relative intensity peak of alumina (at 37.78°). Because of this peak does not appear in batches 1 and 3 for alumina, it could be ascribed to the B_4C coating.

Figure 15b shows the diffractograms of the SiC-coated particles. Cubic SiC (ref. pattern 1-074-2307) is clearly seen in Batch 4. No peaks from the zirconia core are distinguished in this batch. The SiC diffraction peaks in this batch could come from the coating, but the core of the particles of this batch is made of zirconia + carbon/SiC, so it could also come from the external layer of the core. The SiC coating could not be clearly detected in the other batches. Batches 5-8 presented clear peaks from tetragonal ZrO_2 (ref. pattern 42-1164).

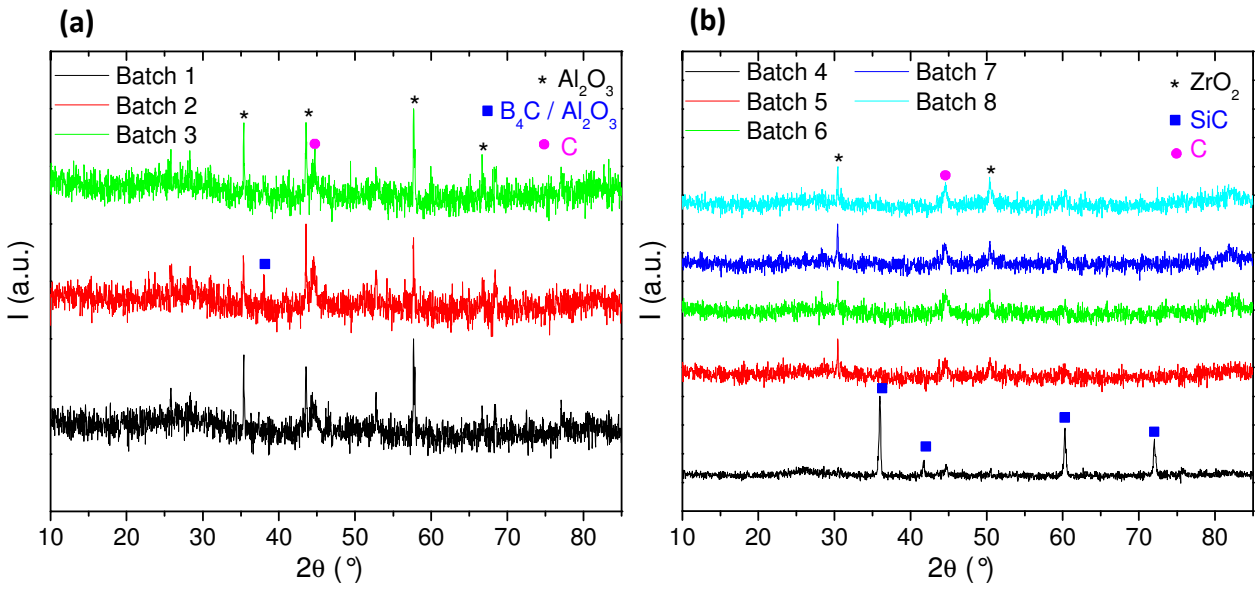

Figure 15. Diffraction patterns of B_4C-coated Al_2O_3 particles (a) and of SiC-coated ZrO_2 particles (b).

2.5. 3D imaging by CT

All batches were scanned by CT, but coatings with a thickness lower than 1 µm could not be resolved. The difference in the grey values of the material and the air background was small due to the low attenuation coefficients of the main elements present in the coatings (B, C, O, Si). As can be seen in the 2D x-ray scans of Batch 4 (Figure 16a), the intermediate carbon layer appears almost transparent (grey value C layer ≈ 8600, grey value background ≈ 8000), and the external SiC layer has a very low contrast (grey value ≈ 11900). The internal zirconia core, the intermediate carbon layer and the external SiC coating could be clearly distinguished after image processing and 3D reconstruction (Figure 16c). A void analysis was performed on the coating with the aim of measuring porosity, but the results were not reliable because the grey value difference between SiC and the possible voids (darker areas within the SiC) was too small.

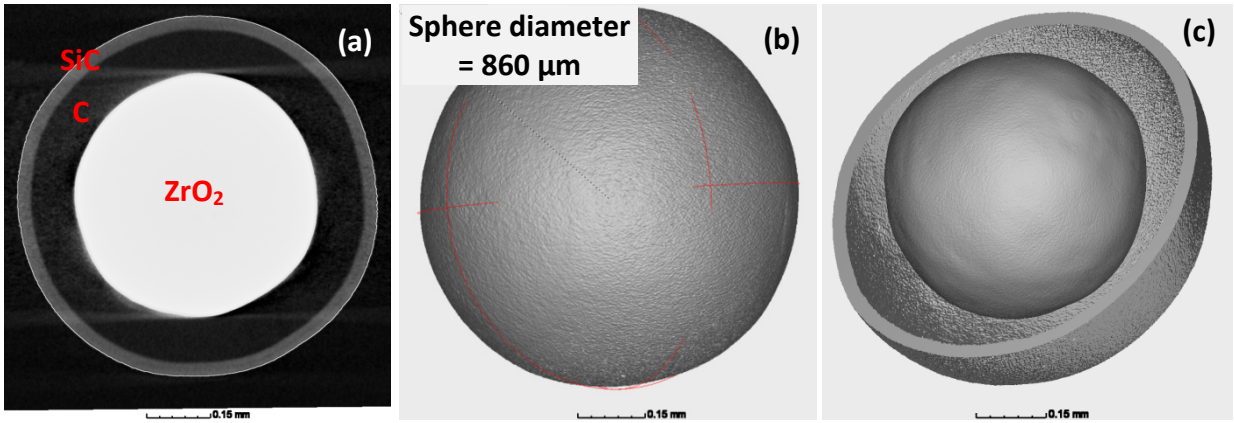

Figure 16. (a) Single 2D x-ray scan of a particle of Batch 4 along its diameter, (b) and (c) show the 3D reconstruction.

The B_4C coatings of Batches 1 and 3 (around 3µm thick) were not seen in the raw CT scans but appeared after a two-step filtering. Figure 17 shows a 2D scan of a particle of Batch 1 before and after image processing. In order to see the coating, the range of grey values was reduced to enhance the contrast at the interface. As a result, the inside of the coating appears with the same grey value, as if it was a monolithic layer. In this situation it was not possible to perform a void analysis to measure the porosity. The 3D reconstruction and wall thickness analysis of this particle are shown in Figure 18. The B_4C coating (Fig. 18a) had a higher roughness than the SiC surface (Fig. 16b) The wall thickness analysis gave a maximum of the thickness histogram at 2.7 µm, close to the 3µm measured by SEM.

The thickness of Batches 2 and 5-8, was too small to be resolved by CT.

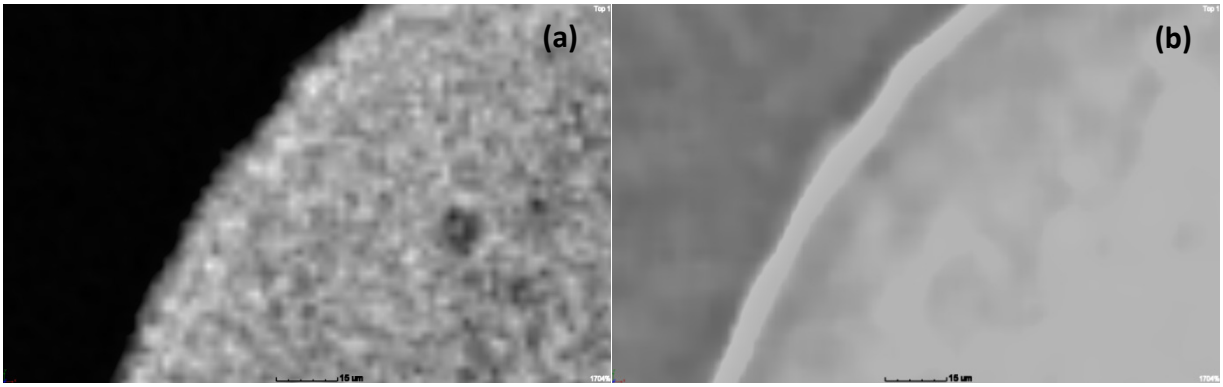

Figure 17. Single 2D x-ray scan of a particle of Batch 1 before (a) and after (b) image processing.

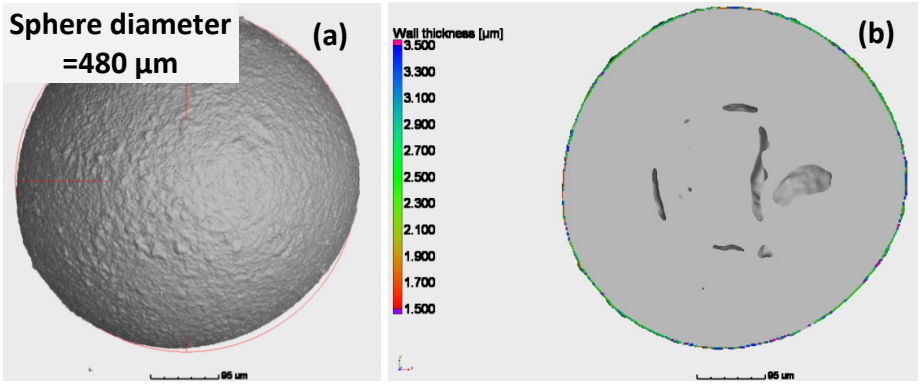

Figure 18. 3D reconstruction (a) and wall thickness analysis (b) of the B_4C coating in Batch 1.

3. PLD optimization

Summary

Eight more batches of B_4C- and SiC-coated micoparticles were produced in the second round of coatings. Four of them (Batches I, II, VII and VIII) consisted of B_4C coatings on Al_2O_3 (I and II) or on buffer/PyC-coated ZrO_2 (VII and VIII). The other four (Batches III – VI) consisted of either Al_2O_3 (III) or of buffer/PyC-coated ZrO_2 (IV – VI) kernels coated with SiC.

The new series of PLD depositions produced coatings of higher quality both for B_4C and for SiC. Table 2 below summarizes the main characteristics of layer thickness and stoichiometry.

The best B/C ratio (3.22) was measured in Batch II, but the thickness of this coating was the lowest among the B_4C (500 nm). On the other hand, Batch I presented a B/C ratio close to 3 and a thickness above 5 µm. Regarding the SiC coatings, all of them presented higher thicknesses than in the previous round (always above 1.5 µm) and the Si/C ratio measured by EDX was close to the stoichiometric value of 1. Moreover, Ag was successfully trapped underneath the SiC coatings, in particular when buffer/PyC-coated ZrO_2 was used as kernel. The highest thickness was observed in Batch V, which also presented a SiC ratio as high as 0.94 and good Ag retention.

As conclusion, **Batch I** for B_4C and **Batch V** for Ag-SiC presented the best properties with regard to layer thickness, stoichiometry and capacity for Ag retention (in the case of SiC).

Table 2. Layer thickness and stoichiometry of the second round of coatings

coating	B_4C				Ag - SiC			
core	Al_2O_3		Buffer/PyC - coated ZrO_2		Al_2O_3	ZrO_2 + buffer + PyC		
Batch ID	**I**	**II**	**VII**	**VIII**	**III**	**IV***	**V**	**VI**
Layer thickness (µm)	5.5	0.5	1.5	1	1.8	1.5	3	2.5
B/C (EDX)	2.99	3.22	0.75	0.31	-	-	-	-
Si/C (EDX)	-	-	-	-	1.02	0.72	0.94	0.86

* no Ag was deposited in Batch IV

3.1. Morphology and layer thickness

3.1.1. B_4C coatings

Figures 19 and 20 present the morphology and thickness, respectively, of the B_4C coatings. The thickest of all B_4C coatings was found in Batch I (5.5 µm). Batch II was very well-packed but too thin (only 500nm). Batches VII and VIII were more porous and thinner than the boron carbide deposited on alumina. Using buffer/PyC-coated zirconia as kernel, the thickness was only slightly above 1 µm, but the layer seemed to adhere better to the PyC substrate than when directly deposited on alumina.

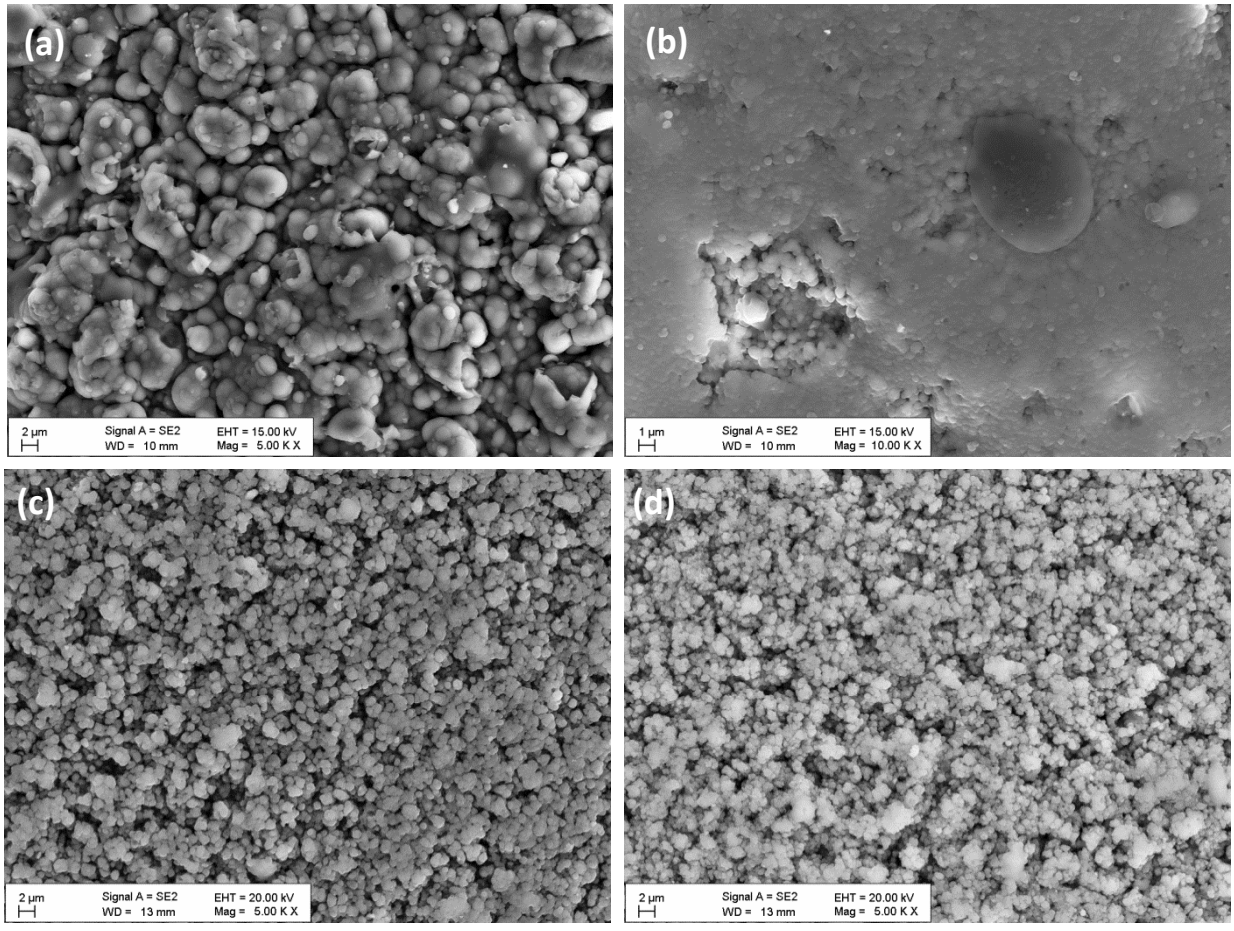

Figure 19. SEM images of the second round of B_4C coatings. Batches I (a), II (b), VII (c) and VIII (d).

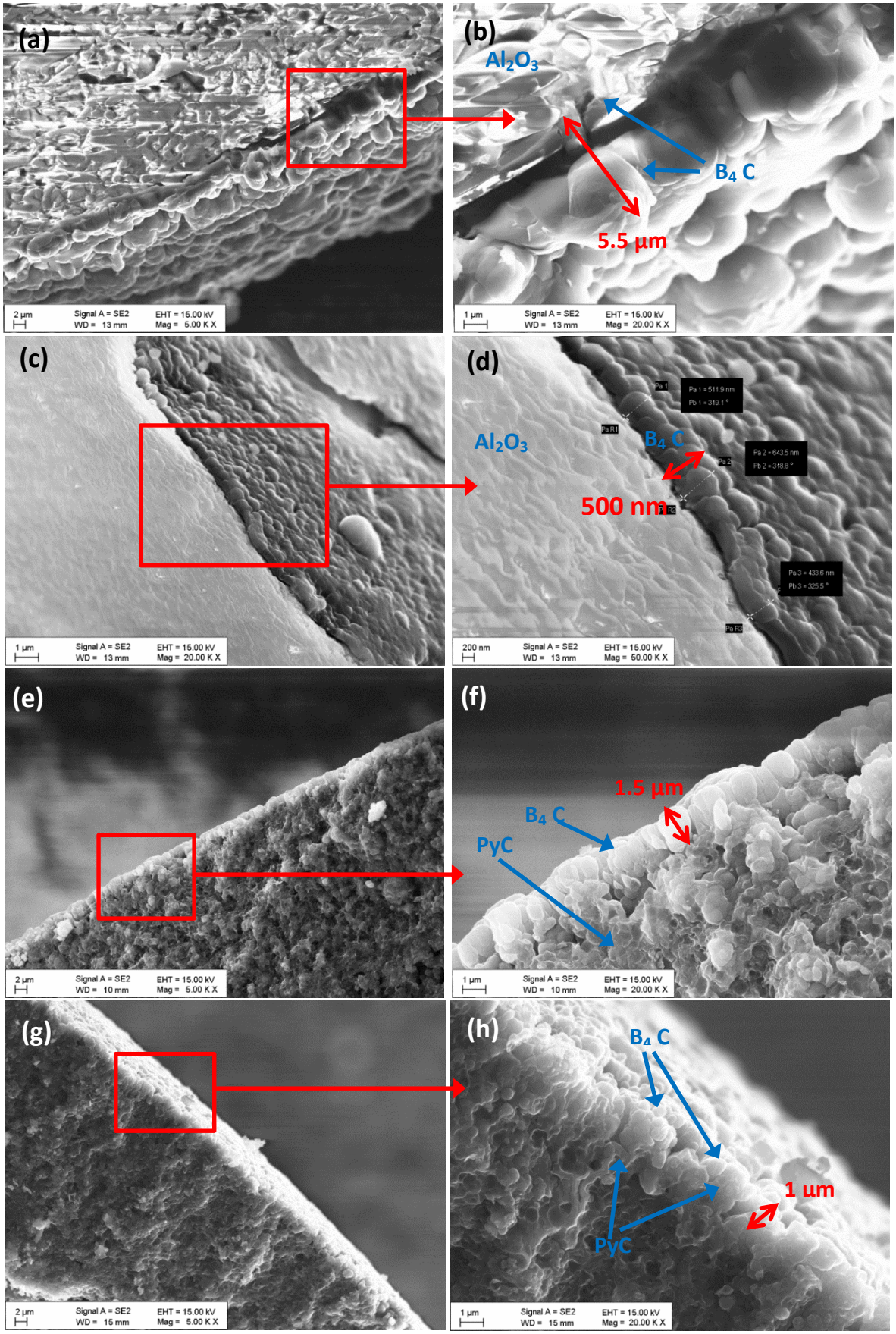

Figure 20. Thickness of the second round of B_4C coatings. Batches I (a,b), II (c,d), VII (e,f) and VIII (g,h). The blue labels indicate the points where EDX was carried out to discern the extension of the coating.

3.1.2. (Ag) - SiC coatings

The morphology of the coating strongly depends on the substrate. The SEM images of the SiC coatings (Figure 21) show that the coatings on PyC (Batches IV-VI) were more porous than the coating on alumina (Batch III). However, the deposition on buffer/PyC-coated ZrO_2 produced thicker coatings (up to 3 µm in Batch V) and, most importantly, the Ag layer was retained between the SiC coating and the kernel, as can be seen in Batches V and VI (Figure 22 f, h).

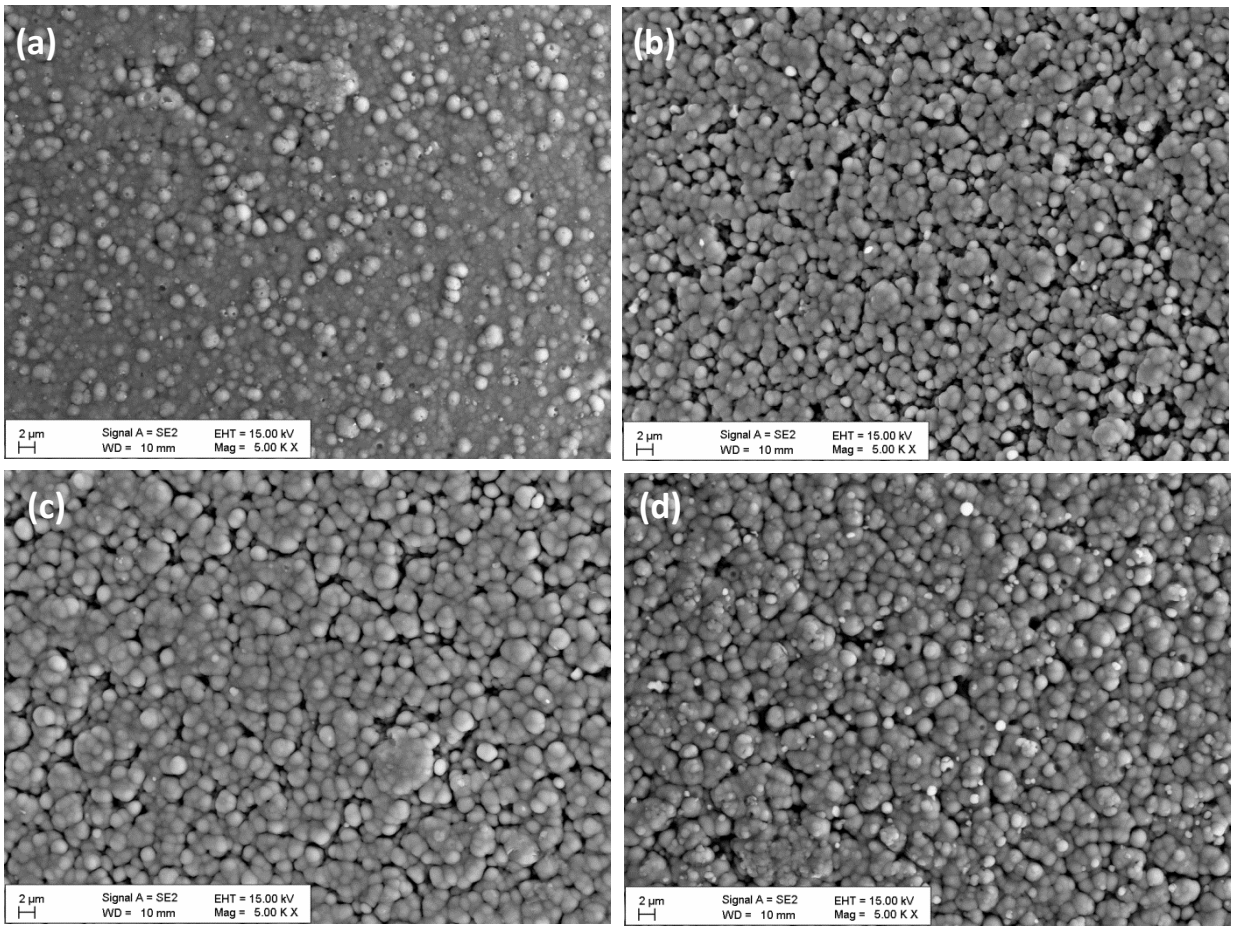

Figure 21. SEM images of the second round of SiC coatings. Batches III (a), IV (b), V (c) and VI (d).

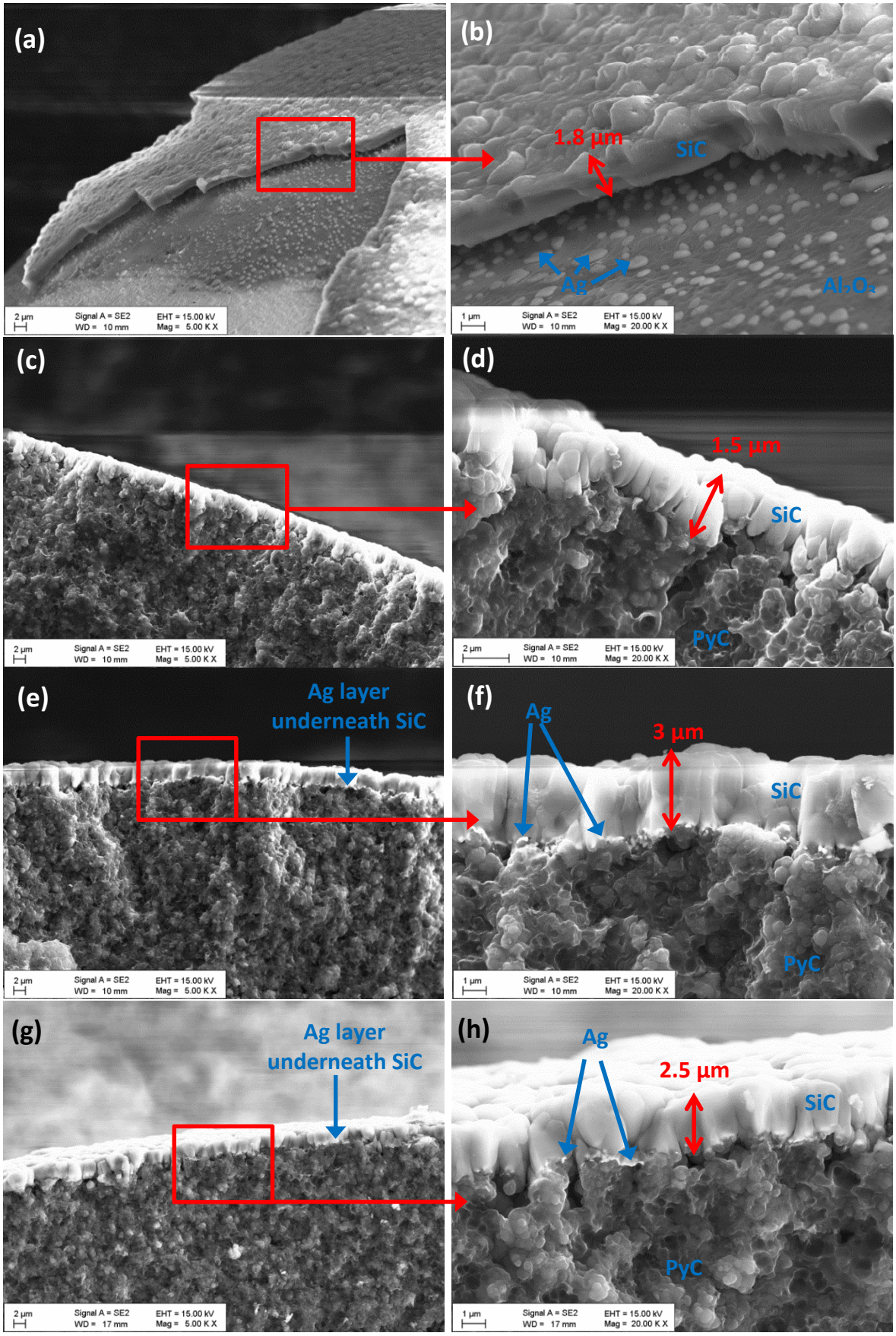

Figure 22. Thickness of the second round of SiC coatings. Batches III (a,b), IV (c,d), V (e,f) and VI (g,h). The blue labels indicate the points where EDX was carried out to discern the extension of the coating.

3.2. Chemical composition

3.2.1. B_4C coatings

The composition analysis of the B_4C coatings (Figure 23) showed that the stoichiometry of Batches I and II is good, slightly improved as compared to the first round. The composition gives a B/C ratio of around 3. On the other hand, the composition analysis of the batches produced on PyC cores gave a high amount of C and, thus, a poor B/C ratio (below 1). The high carbon measured may be due to the contribution of C from the substrate.

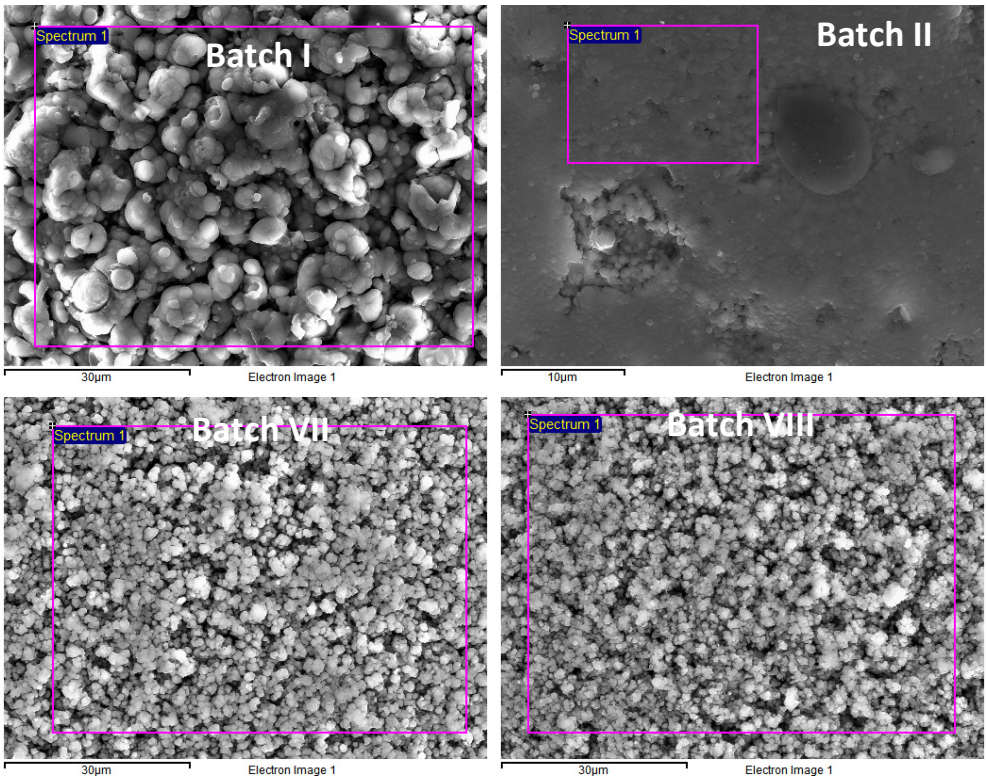

	Composition B_4C coatings (at.%)				
	B	**C**	**O**	**Al**	**B/C**
Batch I	68.46	22.88	7.57	0.73	**2.99**
Batch II	63.31	19.68	8.56	5.45	**3.22**
Batch VII	41.75	55.66	2.59	-	**0.75**
Batch VIII	23.37	75.14	1.49	-	**0.31**

Figure 23. Composition and B/C atomic ratio of the second round of B_4C coatings (Batches I, II, VII and VIII), in at.%.

.

3.2.2. (Ag) - SiC coatings

All SiC coatings exhibited an atomic ratio closer to stoichiometry than in the previous round, with Si/C ratios close to 1. As shown in Figure 24, only carbon, silicon and some oxygen was detected on the surface of the coatings, indicating that diffusion of silver has been prevented and the Ag layer is retained under the SiC. The presence of oxygen might mean that there is some oxidation in the deposited layer, but in Batches IV, V and VI the amount of oxygen is very low (≤ 5 at.%). The higher amount of oxygen in Batch III comes from the contribution of the substrate (alumina in this case). The morphology of the coating strongly depends on the substrate. The coatings on buffer/PyC-coated kernels (Batches IV-VI) are more porous than on alumina (Batch III).

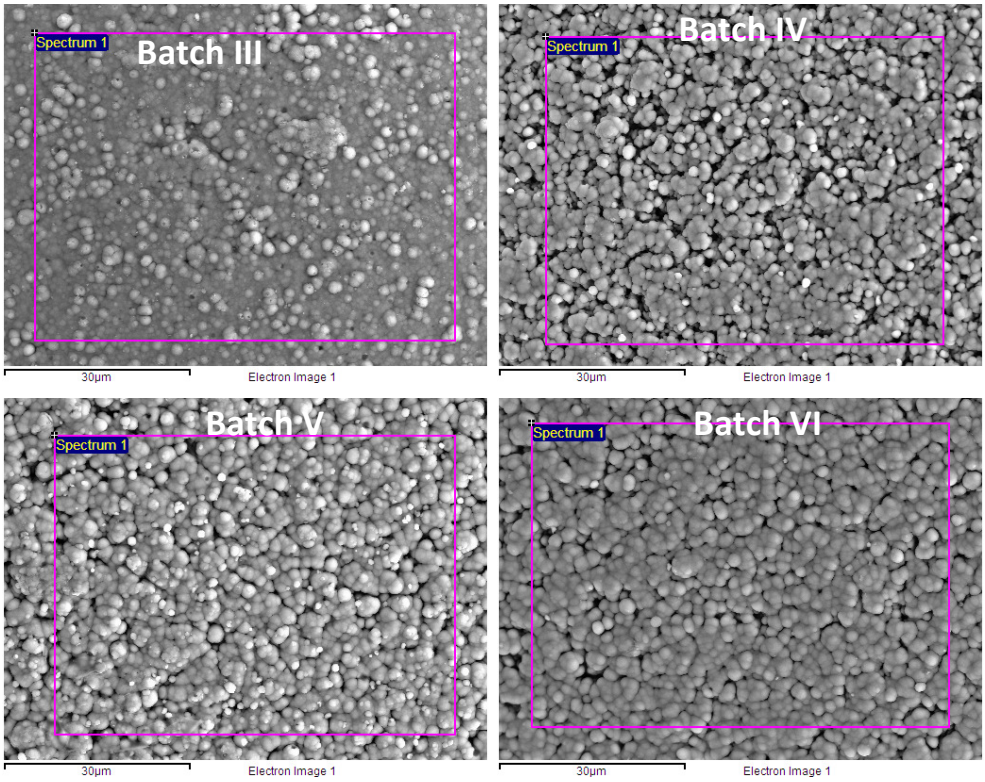

	Composition SiC coatings (at.%)			
	C	O	Si	Si/C
Batch III	40.16	18.73	41.11	**1.02**
Batch IV	55.3	5.02	39.69	**0.72**
Batch V	49.11	4.78	46.11	**0.94**
Batch VI	51.91	3.56	44.54	**0.86**

Figure 24. Composition and Si/C atomic ratio of the second round of SiC coatings (Batches III, IV, V and VI), in at.%.

3.3. Phase analysis by XRD

Figure 25 presents the XRD characterization of the second round of B_4C (a) and SiC (b,c) coatings. Peaks from the Al_2O_3 and the buffer/PyC-coated ZrO_2 kernels are clearly discernible in the XRD signal. For the B_4C coatings, the main peak of B_4C at 37.8° appears in batches I and II, but not in VII and VIII. However this peak cannot be unequivocally ascribed to boron carbide, as it coincides with a peak of the alumina substrate.

In the case of the SiC coatings (Figure 25b), a pronounced peak around 38° appears for the Ag-coated particles of batches III, V and VI, corresponding to the (111) Ag diffraction. However, peaks corresponding to SiC cannot be identified in the diffractograms, even though the thickness of the SiC layer is much higher than the one of the Ag layer. This suggests that the SiC layer is mostly amorphous. A slight peak around 35.6° could be identified by performing a more detailed scan of Batch V in the range from 30° to 65°, indicating that the SiC layer may be at least partially nanocrystalline (Figure 25c).

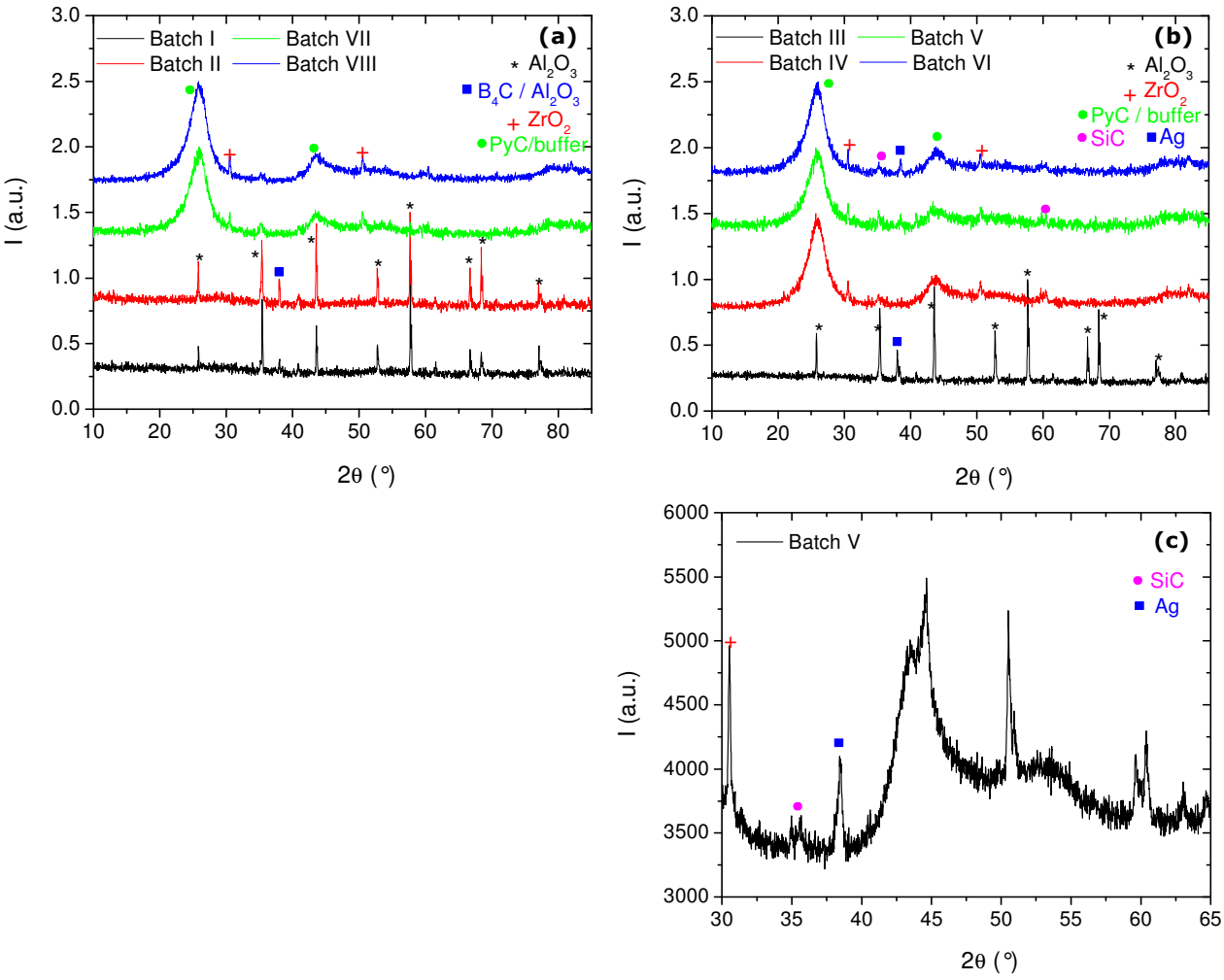

Figure 25. Diffraction patterns of B_4C (a) and SiC (b) coatings. (c) shows a more detailed diffractogram of Batch V taken from 30° to 65°, with step size of 0.01° and 600sec of integration time.

4. Conclusions and Outlook

TRISO-like surrogate kernels delivered by Manchester University have been successfully coated with B_4C and Ag-SiC layers by PLD at Technical University Dresden. Homogeneous coatings of the spherical kernels were achieved by introducing a rotating crucible as holder in the PLD set-up.

The coatings were characterized by JRC-IET in Petten thus enabling the optimization of the PLD process. The best PLD coating for B_4C was produced in Batch I after PLD and surrogate kernel optimization, with a thickness of 5.5 µm and B/C ratio 3. As for Ag/SiC, Batch V after optimization exhibited the best structural and crystallographic characteristics, with a Si/C ratio close to the stoichiometric value of 1, a thickness of 3 µm and an Ag layer buried under the SiC coating.

As a result of this study, it can be confirmed that particles required for separate effect irradiation tests can indeed be fabricated. This will allow further progress in fuel performance assessment which is a required step in the licensing procedure of a future HTR demonstrator.